Paul Dallavalle

WEATHER BUREAU
Office of Systems Development
Techniques Development Laboratory
Silver Spring, Md.

October 1968

Prediction of Temperature and Dew Point by Three-Dimensional Trajectories

Ronald M. Reap

Technical Memorandum WBTM TDL 15

U.S. DEPARTMENT OF COMMERCE / ENVIRONMENTAL SCIENCE SERVICES ADMINISTRATION

WEATHER BUREAU TECHNICAL MEMORANDA

Techniques Development Laboratory

The primary purpose of the Techniques Development Laboratory of the Office of Systems Development is to translate increases in basic knowledge in meteorology and allied disciplines into improved operating techniques and procedures. To achieve this goal, TDL conducts and sponsors applied research and development aimed at improvement of diagnostic and prognostic methods for producing weather information. The laboratory carries out studies both for the general improvement of prediction methodology used in the National Meteorological Service System and for more effective utilization of weather forecasts by the ultimate user.

Weather Bureau Technical Memoranda in the Techniques Development Laboratory series facilitate rapid distribution of material which may be preliminary in nature and which may be published formally elsewhere at a later date. Weather Bureau Technical Memoranda are a continuation of the former Weather Bureau Technical Notes series which included TDL-1 through TDL-5.

Papers listed below are available from the Clearinghouse for Federal Scientific and Technical Information, U.S. Department of Commerce, Sills Bldg., 5285 Port Royal Road, Springfield, Va. 22151. Price: $3.00 hard copy; $0.65 microfiche. Order by accession number shown in parentheses at end of each entry.

TN 10 TDL 1 Objective Prediction of Daily Surface Temperature. William H. Klein, Curtis W. Crockett, and Carlos R. Dunn, October 1965. (PB-168 590)

TN 11 TDL 2 Hurricane Cindy Galveston Bay Tides. N. A. Pore, A. T. Angelo, and J. G. Taylor, September 1965. (PB-168 608)

TN 29 TDL 3 Atmospheric Effects on Re-Entry Vehicle Dispersions. Karl R. Johannessen, December 1965. (PB-169 381)

TN 45 TDL 4 A Synoptic Climatology of Winter Precipitation from 700-mb. Lows for the Intermountain Areas of the West. D. L. Jorgensen, W. H. Klein, and A. F. Korte, May 1966. (PB-170 635)

TN 47 TDL 5 Hemispheric Specification of Sea Level Pressure from Numerical 700-mb. Height Forecasts. William H. Klein and Billy M. Lewis, June 1966. (PB-173 091)

WBTM TDL 6 A Fortran Program for the Calculation of Hourly Values of Astronomical Tide and Time and Height of High and Low Water. N. A. Pore and R. A. Cummings, January 1967. (PB-174 660)

WBTM TDL 7 Numerical Experiments Leading to the Design of Optimum Global Meteorological Networks. M. A. Alaka and F. Lewis, February 1967. (PB-174 497)

WBTM TDL 8 An Experiment in the Use of the Balance Equation in the Tropics. M. A. Alaka, D. T. Rubsam, and G. E. Fisher, March 1967. (PB-174 501)

WBTM TDL 9 A Survey of Studies of Aerological Network Requirements. M. A. Alaka, May 1967. (PB-174 984)

WBTM TDL 10 Objective Determination of Sea Level Pressure from Upper Level Heights. William Klein, Frank Lewis, and John Stackpole, May 1967. (PB-179 949)

WBTM TDL 11 Short Range, Subsynoptic Surface Weather Prediction. H. R. Glahn and D. A. Lowry, July 1967. (PB-175 772)

WBTM TDL 12 Charts Giving Station Precipitation in the Plateau States from 700-Mb. Lows During Winter. D. L. Jorgensen, A. F. Korte, and J. A. Bunce, Jr., October 1967. (PB-176 742)

WBTM TDL 13 Interim Report on Sea and Swell Forecasting. N. A. Pore and W. S. Richardson, December 1967. (PB-177 038)

WBTM TDL 14 Meteorological Analysis of 1964-65 ICAO Turbulence Data. DeVer Colson, September 1968. (PB-)

UDC 551.509.323 + 551.571.3:551.509.326:551.509.313

12/8/74

U.S. DEPARTMENT OF COMMERCE
Environmental Science Services Administration
Weather Bureau

Weather Bureau Technical Memorandum TDL 15

PREDICTION OF TEMPERATURE AND DEW POINT BY THREE-DIMENSIONAL TRAJECTORIES

Ronald M. Reap

OFFICE OF SYSTEMS DEVELOPMENT
TECHNIQUES DEVELOPMENT LABORATORY

SILVER SPRING, MD.
October 1968
Reprinted April 1971

CONTENTS

PREDICTION OF TEMPERATURE AND DEW POINT BY THREE-DIMENSIONAL TRAJECTORIES

By

Ronald M. Reap
Techniques Development Laboratory
Weather Bureau, ESSA
Silver Spring, Maryland 20910

ABSTRACT

A numerical model is developed to compute three-dimensional trajectories from operational wind forecasts generated by the six-layer primitive equation model of the National Meteorological Center. Detailed forecasts of temperature and dew point, designed for application to severe storm prediction, are subsequently derived by computing the six-hourly variations of potential temperature and mixing ratio for air parcels assumed to follow paths defined by the trajectories. Initial values at the trajectory origin points are provided by an objective analysis technique which is capable of reproducing detailed patterns and gradients with only light smoothing of the observations. The influence of a relatively detailed terrain is also included in the program. Verification statistics for 74 test cases run during May-July 1968 indicate a significant improvement over the primitive equation model forecasts in the lowest 150 mb, where temperature and moisture distributions are crucial to severe storm development. Good agreement was also observed between the forecast dew point gradients and severe weather as viewed by the ESSA 3 satellite.

1. INTRODUCTION

The basis for achieving accurate local area forecasts often rests upon the ability of the forecaster to project rapidly changing fields of meteorological variables forward in time and space from current mesoscale analyses. This objective is seldom realized in actual practice due to a number of varied and complex requirements. Among the prime requirements is the need for a fine-mesh dynamic model which is capable of generating realistic mesoscale forecasts, including boundary layer interactions with the large-scale environment. In addition to the theoretical problems involved, such a model would also require frequent and detailed observations from a dense network of surface and upper-air stations. Since the above information is currently not obtainable within the framework of existing data networks and meteorological capabilities, the present research is of necessity directed toward a more limited objective.

The specific aim of the current effort is to attain greater accuracy and detail in the prognosis of three-dimensional temperature and moisture distributions below 500 mb. Improved forecasts of this type would have a potential application to many related meteorological problems requiring derived parameters such as areal cloud coverage, cloud ceiling, and precipitation. However, the principal effort in the present research is directed toward the problem of supplying useful guidance in the domain of severe storm prediction. Since the behavior of mesoscale systems is intimately related to larger scale circulations, it is possible to formulate sub-synoptic predictors from detailed forecasts of temperature and moisture. In adopting this approach to the severe storm problem, it must be emphasized that only general areas of possible or probable severe storm occurrence can be delineated by derived predictors or indices.

The underlying feature of the present research involves the computation of three-dimensional trajectories from an auxilliary program which does not interact with but utilizes operational wind forecasts generated by the six-layer primitive equation model (Shuman and Hovermale, 1968) currently in operation at the National Meteorological Center (NMC). Forecasts are subsequently prepared by following the variations of temperature and moisture along the trajectories. Since the trajectories represent integrated three-dimensional motions of the atmosphere, they relate closely to observed weather. Recent studies by Rogers and Sherr (1967), Nagle and Clark (1966), and Danielsen (1966) have re-emphasized the fact that cloud patterns, and of course attendant convection, evolve in a Lagrangian manner. A cloud forecast model based on this concept has been under continuous development since 1962 by the Air Weather Service, USAF . As shown by Edson, et al. (1967), significant improvements have been achieved in the accuracy of temperature and moisture forecasts, from which automated cloud forecasts are routinely prepared. One of the principal reasons for the success of the Lagrangian approach is that it inherently provides superior resolution of forecast fields due to an absence of the cumulative truncation errors found in Eulerian computations. Errors of this type can be especially significant when one considers the high degree of spatial and temporal variability that is found in low-level temperature and moisture distributions prior to and during severe storm conditions.

However, trajectories are subject to various inaccuracies. As indicated by Djuric (1961), the major errors in objectively computed trajectories lie in the choice of the theoretical approximation to the actual wind and in the sparsity of observed data in most parts of the world. In a study of flights by radar-tracked constant-volume balloons, Peterson (1966) found that low-level trajectories constructed from the surface geostrophic wind are less representative of the boundary layer flow than those computed from an adjusted surface wind. Similarly, Angell (1960) found significant ageostrophic motions at 300 mb, as deduced from long-range flights of constant-pressure balloons. The extreme sensitivity to the wind approximation was revealed by a series of trajectory hindcasts made by Djuric (1961) using identical 300-mb geopotential data in conjunction with three different geostrophic or stream function approximations to the nondivergent wind. In only 12 hours, the mean displacement error between the trajectory end points ranged up to 20 percent of the trajectory length. These differences were nearly equal in magnitude to the individual deviations from the actual end points as measured by tracking flights of constant-pressure balloons.

Errors arising from sparse data distributions are minimized in the present study since the forecasts are prepared for the relatively data-rich continent of North America. However, it must be noted that some of the trajectories which terminate over land may originate from oceanic regions having few nearby observations. Significant errors can result in such cases, depending of course to a large extent on the homogeneity of the source region.

It appears obvious from the above considerations that the nondivergent wind does not accurately reflect the actual wind. Therefore, it is desirable and indeed necessary to tie any trajectory forecast scheme to a prognostic model which incorporates a more realistic wind approximation. Linking the trajectory computations to the NMC primitive equation model effectively utilizes an excellent wind approximation since the nongeostrophic or "raw" u, v, and w wind components are computed directly from the equations of motion and not as by-products from the stream fields. In addition, the feedback of latent-heat and radiational heating and cooling in the primitive equation model, coupled with an improved vertical resolution in comparison to previous operational models, has resulted in more realistic wind forecasts. This is especially true for the lowest 150 mb of the atmosphere where flow patterns are crucial to the development of severe storms.

2. TRAJECTORY COMPUTATIONS

Input data to the trajectory program consist of six-hourly wind forecasts for the 1000, 850, 700, 500, and 300 mb pressure levels. The data are processed by the CDC 6600 computer at Suitland, Md., and stored on tape for the 26x33 grid of points shown in Fig. 1. The horizontal grid length of 381 km is identical to that used at NMC.[1] Considering only one-dimensional displacements and noting that the trajectories are computed backwards from selected terminal points to origin points, the computation procedure is outlined as follows:

[1] At 60°N on a 1:30,000,000 polar stereographic projection.

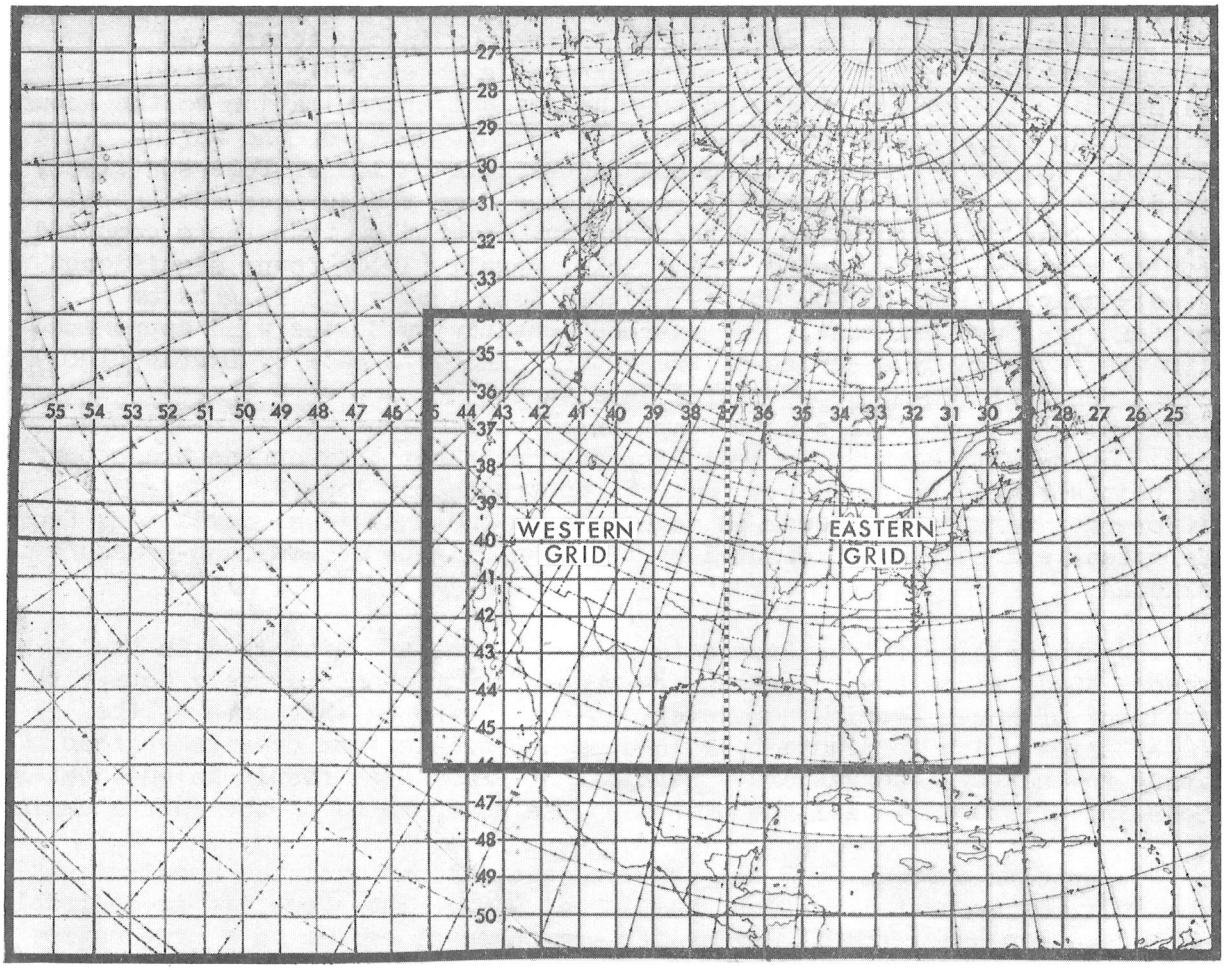

Figure 1. - Grid array for which wind forecasts from the NMC primitive equation model are stored. The grid interval is 381 km at 60°N. Trajectories terminate at grid points given by the 13x17 array centered over the United States. Temperature and dew point forecasts are verified separately for the eastern and western grids.

A first-guess position is obtained from

$$X_2(t-\delta t) = X_1(t) - u_1(t)\delta t \qquad (1)$$

where $X_2(t-\delta t)$ is the origin or upwind point, $u_1(t)$ is the wind component at the terminal point $X_1(t)$ and δt is the time increment for trajectory iterations. After extensive testing, a value of δt=2 hr was chosen to insure a good compromise between the desired accuracy and computer time. The second approximation to the location of the trajectory origin point is given by

$$X_3(t-\delta t) = X_1(t) - \frac{\delta t}{2}\left[u_2(t-\delta t) + u_1(t)\right] \qquad (2)$$

where $u_2(t-\delta t)$ is interpolated to the point $X_2(t-\delta t)$. Successive iterations of (2) are performed by replacing $u_2(t-\delta t)$ with $u_3(t-\delta t)$, as interpolated to $X_3(t-\delta t)$, etc., until the trajectory origin points converge within prescribed limits. Typical values for the horizontal and vertical convergence criteria are 0.1 grid interval and 1.0 mb. Trajectories outside the grid in the horizontal or vertical are terminated at the lateral boundaries or at 300 mb. Interpolations in the vertical and in time between successive prognostic fields of the wind components are given by

this is the interpolation for $u_2(t-\delta t)$ in time or vertical space

$$f(X_o+\phi h) = \frac{\phi(\phi-1)}{2} f_{-1} + (1-\phi^2) f_o + \frac{\phi(\phi+1)}{2} f_1 \qquad (3)$$

(h can refer to time or vertical dimension)

where $f_o=f(X_o)$, $f_{-1}=f(X_o-h)$, $f_1=f(X_o+h)$ are the values of the wind components for three consecutive six-hourly forecasts or standard pressure levels. The interval between f_o, f_{-1}, and f_1 is given by h and ϕ is defined as the fraction of h between f_o and the point of interpolation. A four point bi-linear formula is used for interpolations on the standard pressure levels. } hr. interp. Initial vertical velocities are approximated by backward advection of the six-hour forecast fields. This procedure is desirable since vertical velocities in the primitive equation model are initially set to zero by the use of nondivergent winds computed from the balance equation.[2]

Examples of 36-hr trajectories are given in Fig. 2. Note the differences in the point of origin between the three-dimensional and corresponding isobaric trajectories. These differences reflect the important role played by the large-scale vertical velocities in transporting air parcels through horizontal wind fields of varying speed and direction. According to Danielsen (1961), in extreme but not impossible cases having large vertical wind shears, horizontal deviations up to 1000 km in 12 hours can be observed between isobaric and isentropic trajectories.

As a further refinement, the influence of a relatively detailed terrain representation is incorporated into the trajectory program. The terrain is defined on a grid with a mesh length of approximately 120 miles, or one-half that of the NMC mesh. The terrain heights shown in Fig. 3 are expressed in terms of pressure and are based on the ICAO standard atmosphere relation P=1013-0.1065Z, where Z is the terrain height in meters averaged for overlapping 1 deg latitude by 1 deg longitude squares. At the conclusion of each time step the trajectory height is compared to the interpolated terrain height at the new parcel location. The trajectories are not allowed to intersect the earth's surface and are systematically displaced by the terrain. Examples of the effects of terrain upon low-level trajectories are given in

---

[2] Effective April 29, 1968, the divergent wind component from the previous 12-hr forecast was added to the balanced wind field to provide initial vertical motions.

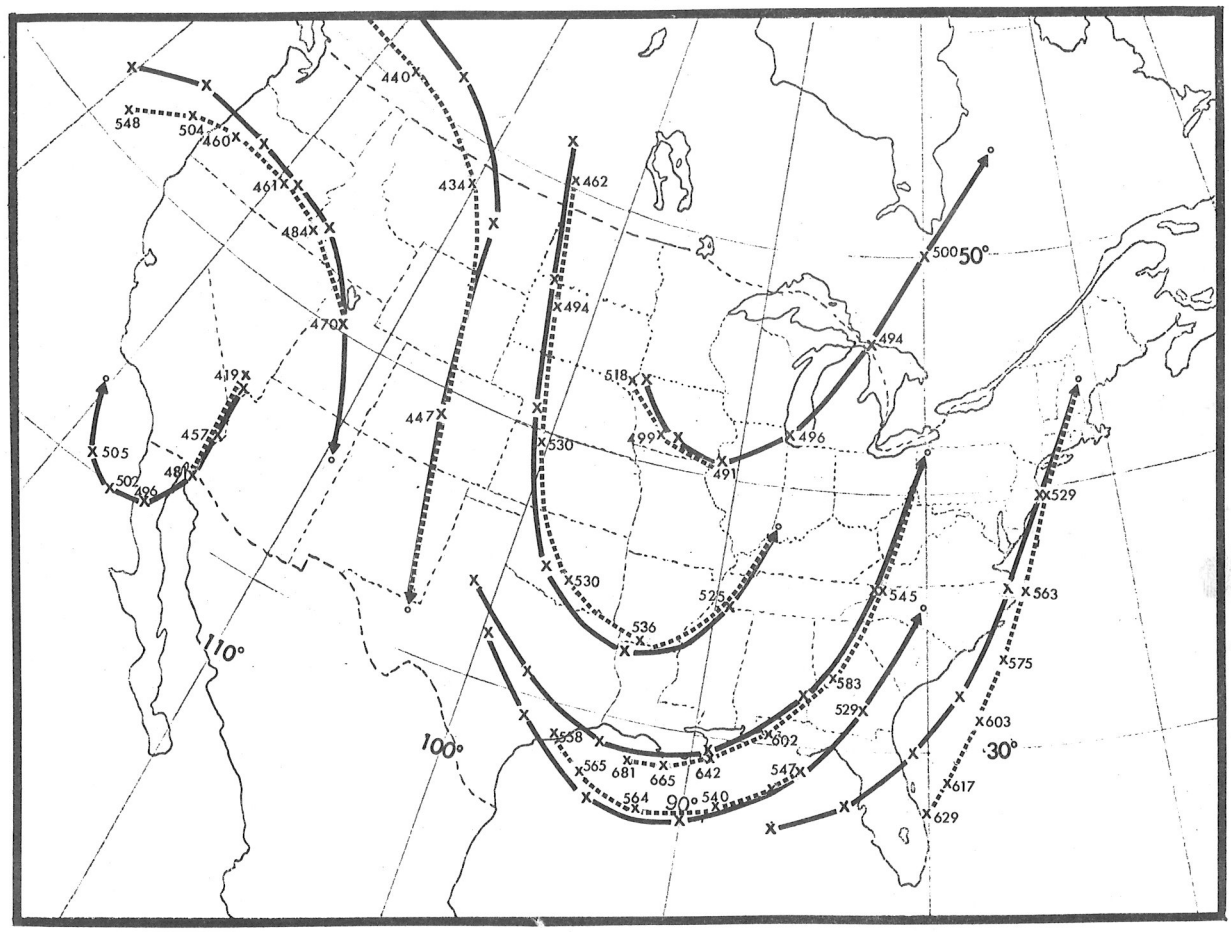

Figure 2. - Dashed lines represent 36-hr three-dimensional trajectories ending at 1200 GMT November 2, 1966. Isobaric trajectories for the same period are denoted by solid lines. All trajectories terminate at 500 mb with pressures given at 6-hr intervals.

Figs. 4-5. From the examples it is clearly seen that under favorable synoptic conditions, simulated air parcels can undergo considerable vertical displacement and thermodynamic modification.

3. OBJECTIVE ANALYSIS

Since the three-dimensional trajectories are computed backwards from forecast points to origin points, it is necessary to specify the state of the initial temperature and moisture fields. Keeping in mind the importance of sub-synoptic features to the development of severe storms, an appropriate analysis technique, i.e., one which is capable of reproducing detailed patterns and gradients with only light smoothing of the observations, was integrated into the trajectory program to provide analyzed values of temperature and moisture at the trajectory origin points. The objective technique selected was originally developed by Endlich and Mancuso (1968) to study various synoptic conditions associated with severe storm occurrence. Their analysis procedure is specifically designed to analyze winds,

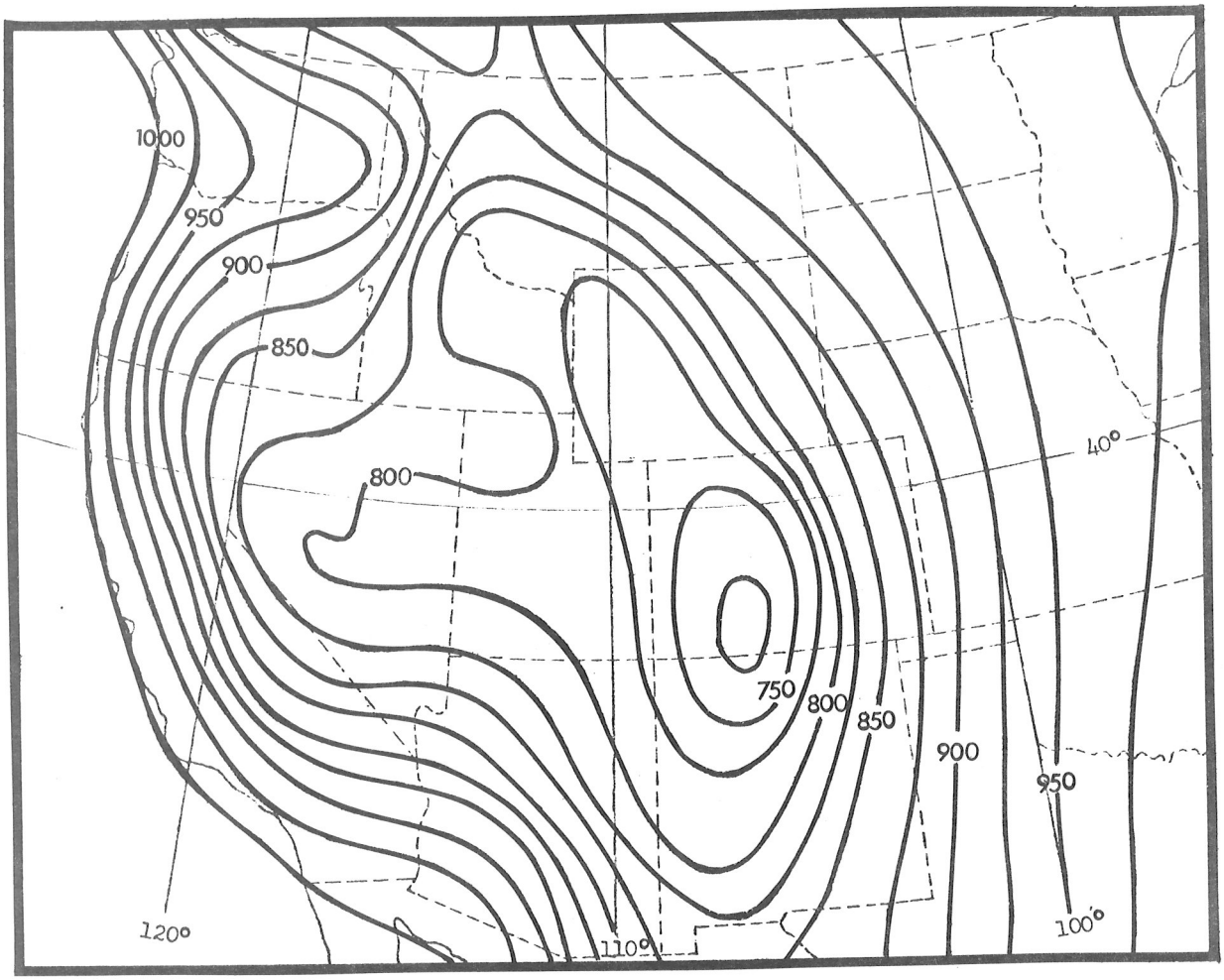

Figure 3. - A portion of the smoothed topography utilized in the computation of low-level trajectories. The terrain heights (mb) are averaged for overlapping 1 deg latitude by 1 deg longitude squares.

temperatures, and dew points at individual points in contrast to conventional methods of analysis which are primarily concerned with hemispheric synoptic-scale motions derived from smoothed fields of pressure-height data. The former approach is desirable in the present research since the trajectory origin points are distributed rather unevenly in three-dimensional space. The present approach also eliminates the need for selecting the appropriate grid lengths required for temperature and dew point analyses at several levels.

Information supplied to the objective analysis scheme consists of standard upper-air data and positions for the trajectory origin points. RAOB data for the 26x33 grid (Fig. 1) are extracted from the NMC automatic data processing (ADP) tapes. Temperatures and dew points for mandatory and significant levels are combined in consecutive order. If necessary, the reproduced soundings can be printed-out for visual checking and comparison. The analysis procedure obtains the analyzed values by fitting a plane surface by least squares to five observations nearest a trajectory origin point.

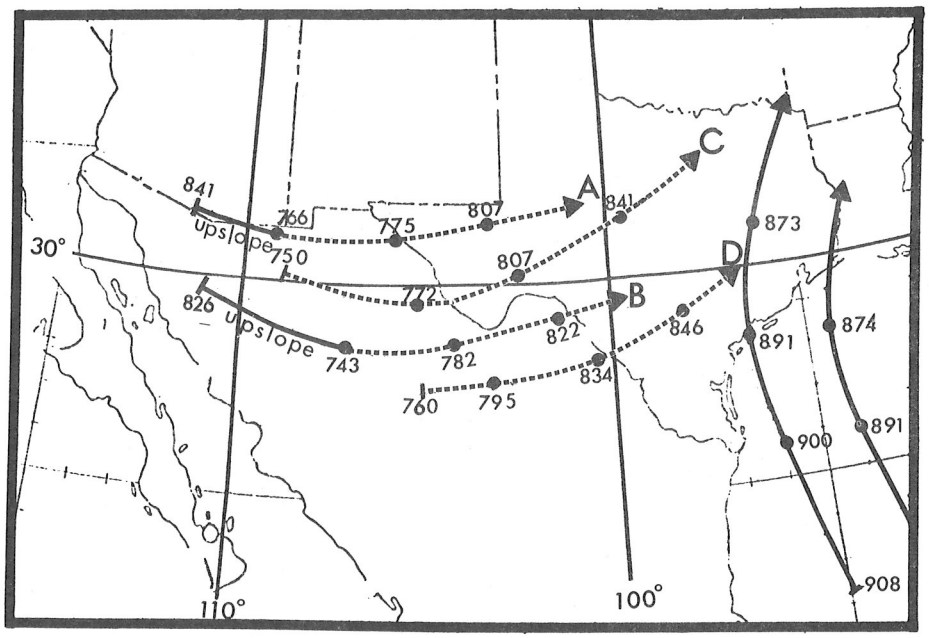

Figure 4. - Plan view of 24-hr trajectories terminating at 850 mb. Solid (dashed) lines represent rising (subsiding) motion with pressures given at 6-hr intervals. Severe weather was associated with the pattern of confluent flow in eastern Texas. Trajectories labeled A, B, C, and D also appear in Fig. 5.

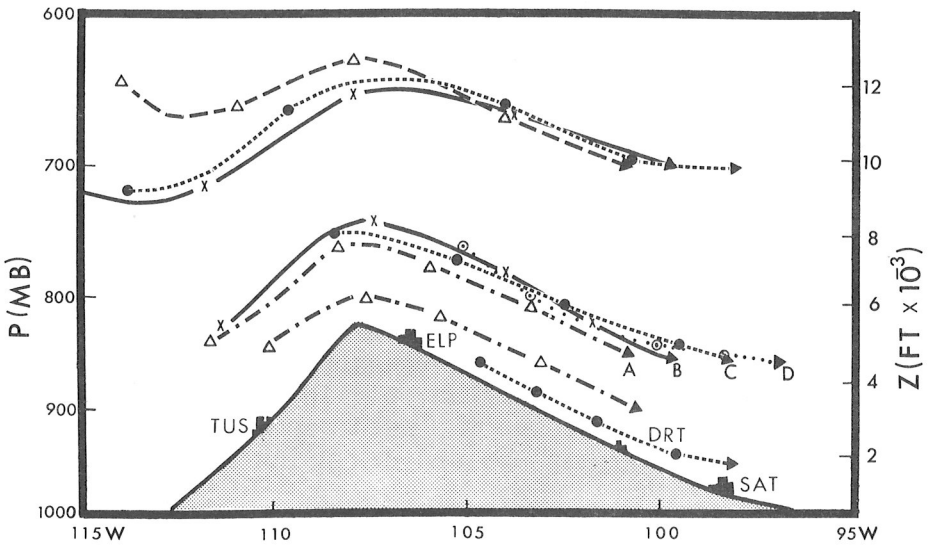

Figure 5. - Vertical cross-section along 30°N. The 6-hr vertical displacements clearly reflect the simplified modeling concept used to simulate the mountain perturbation, i.e., allowing the perturbation to decrease linearly from a maximum at the surface to zero at 600 mb.

The temperature and dew point for each observation is linearly interpolated from mandatory or significant data points vertically adjacent to the level of the trajectory origin point. In addition, the temperature lapse rate between the selected data points is error-checked to eliminate any observations with superadiabatic lapse rates or unrealistically large inversions. A distance weighting factor for each observation is introduced prior to the fitting process to avoid excessive smoothing. The weighting factor is given by

$$W = C^2 \left[(R+R^*)^2 + C^2 \right]^{-1} \qquad (4)$$

where C^2 is a constant, R is the magnitude of the position vector $\underline{R}$ from the trajectory origin point to the observation and R* is a distance factor given by the magnitude of $\underline{k} \circ \underline{R} \times (\underline{V}/V)$ and computed as

$$R^* = (v.x - u.y)/(u^2+v^2)^{1/2} \; ; \qquad R \geq R^* \geq 0 \qquad (5)$$

where u and v are wind components interpolated to the observation and x and y are the scalar components of $\underline{R}$. The distance factor (R*) is used to give upwind-downwind observations greater weight than crosswind observations. Isolines of the analyzed scalar are more closely aligned with the flow direction as a result of this correction. This feature, while typical of the entire troposphere, is especially consistent with numerous observations by severe storm forecasters which reveal the existence of well-defined temperature and moisture axes parallel to the low-level flow. The effect of the distance factor is indicated by the weighting curves in Fig. 6 where C^2=0.75 and R* varies between R and 0. For comparison, the dashed lines approximate the range of the weighting factor $W=(N^2-R^2)/(N^2+R^2)$ used at NMC. As given by Cressman (1959), R is the distance between the grid point and the observation and N is the distance at which W goes to zero.

4. PARCEL THERMODYNAMICS

The final step in the forecast procedure is accomplished by computing the changes in temperature and moisture, according to known physical laws, for air parcels moving along the three-dimensional trajectories. Subsequent to determining the initial values of potential temperature (θ) and mixing ratio (M) at the trajectory origin points, the program computes the six-hourly variations of these quantities for parcels assumed to move along paths defined by the trajectories. Each parcel rises (or descends) dry-adiabatically provided the computed mixing ratio deficit (M_d) remains positive during the six-hour period, where $M_d=M_s-M$ and M_s is the saturation mixing ratio. If saturation occurs, as indicated by a negative M_d at the end of the six-hour period, the program backs up and computes the lifting condensation level (LCL) temperature and pressure. The parcel in this case is lifted dry-adiabatically to the LCL and pseudo-adiabatically thereafter. Since the LCL is defined as the intersection point between the mixing ratio line and the constant potential temperature line, an iterative procedure, partly devised by Stackpole (1967), is used to solve for the LCL pressure in

Mixing Ratio $\overset{\text{def}}{=} \frac{\text{mass of vapor}}{\text{mass of dry air}} = \frac{M_v}{M_d} \approx .622 \frac{e}{p}$

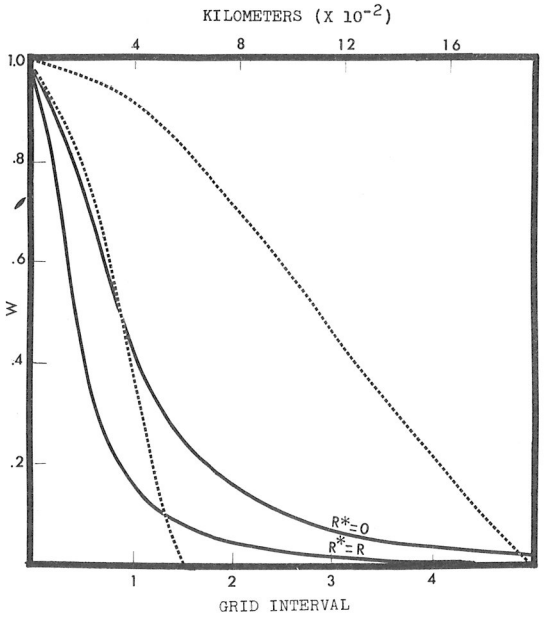

Figure 6. - Weighting curve (W) as a function of distance from observation (R) and the distance factor (R*). Dashed lines represent the NMC weighting curve $W=(N^2-R^2)/(N^2+R^2)$, for N=1.5 and N=5.0.

a rapid and economical manner. As determined from numerous tests, the procedure gives results which are identical to those obtained from similar graphical computations.

The equation utilized by the program to describe the pseudo-adiabatic process was defined by Rossby (1932) and is given by

Hess p.56

$$\theta_{PE} = \theta_P \exp(LM/C_pT) \tag{6}$$

where θ_{PE} is the pseudo-equivalent potential temperature, θ_P is the partial potential temperature given by $T(1000/P-e)^{0.286}$, L is the latent heat of condensation, M is the mixing ratio, C_p is the specific heat of air at constant pressure, T is the temperature at saturation, P is the total pressure, and e is the vapor pressure. The solution of (6) for the new parcel temperature T_2, at the pressure level P_2 given by the trajectory, is accomplished by employing a numerical algorithm similar to one constructed by Stackpole (1967). From the temperature (T_{LCL}) and pressure (P_{LCL}), at the lifting condensation level, we can obtain θ_{PE}, which is constant along the pseudo-adiabat intersecting the LCL point. T_2 is then computed in an iterative manner using the relation

$$D = \theta_P \exp(LM_s/C_pT_2) - \theta_{PE}(T_{LCL}, P_{LCL}) \tag{7}$$

where D is the difference or error between successively better estimates of T_2. The procedure is terminated when D<E, where E is the maximum allowable error of .05K. The saturation mixing ratio at T_2 is given by $M_s=0.622(e_s/P-e_s)$ where e_s is the saturation vapor pressure computed from Teten's equation as described by Murray (1967).

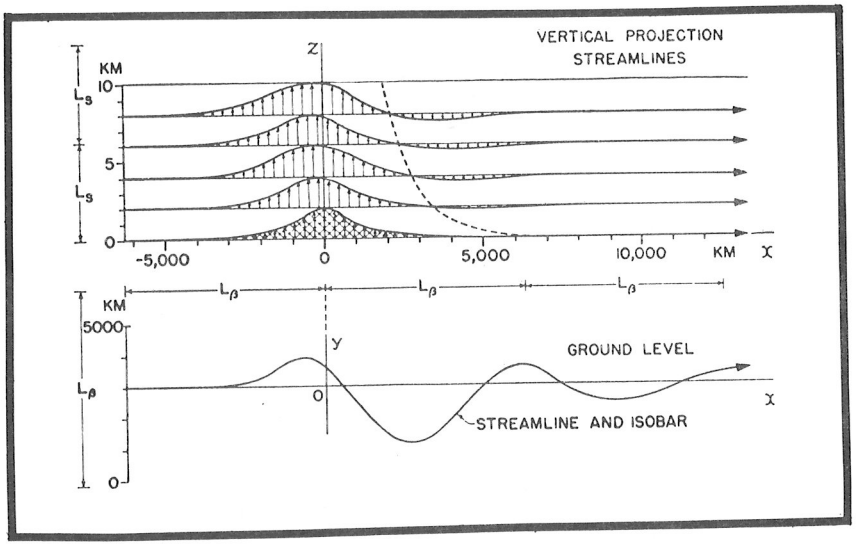

Figure 7. - Perturbation by a very broad typical mountain range in an unlimited uniform stratified westerly wind (u=10 m/s). Upper part: vertical projection of the streamlines; displacement indicated by small arrows. Lower part: horizontal projection of a streamline at ground level (after Queney).

5. OROGRAPHIC EFFECTS

In regions of sloping terrain, the air immediately above the surface is subjected to forced vertical motion. An accurate determination of the air flow above the contact layer will then become quite complicated. A simplified treatment of the problem, namely the behavior of frictionless air flow across a broad mountain barrier, similar to the one given in Fig. 5, was discussed by Queney (1948). As shown by Fig. 7, his model indicated that at all heights the vertical projection of the streamlines closely follows the mountain profile. The large horizontal deflections in the streamlines are due to the dynamic effect of the earth's rotation. One of the important limitations of the model is the assumption that $\partial V_x/\partial Z=0$, where V_x is a uniform current normal to the mountain range. Introduction of the usual vertical wind shear found in the mid-latitude westerlies results in pronounced damping of the vertical streamline amplitude with height.

Keeping in mind the above considerations, the NMC vertical velocities at low levels over the western mountains were replaced by terrain-induced displacements obtained from a simplified model which is more responsive to the detailed terrain (Fig. 3) used in the trajectory program. At this point it must be noted that the terrain given in Fig. 3 represents a significant improvement over that presently used in the primitive equation model, as given by Berkofsky and Bertoni (1955).[3] The topographic gradients and positioning of major terrain features are found to differ considerably in many areas. An essential feature of the simplified model is the assumption

[3]Testing is currently underway at NMC to determine the feasibility of incorporating a more detailed terrain into the primitive equation model.

of a linear decrease of the mountain perturbation from a maximum at the surface to zero at 600 mb. As illustrated by Fig. 5, air parcels near the surface closely follow the terrain, while parcels at intermediate heights undergo less vertical displacement. [Parcel displacements above 600 mb are entirely controlled by large-scale vertical motions, which of course implicitly contain a terrain-induced component.] The horizontal boundaries of the mountain perturbation, outside of which the vertical displacements are determined only by large-scale vertical motions, are taken as the 1000-mb contour along the west coast of the United States and the 950-mb contour along 100°W, as shown by Fig. 3.

6. EVALUATION OF RESULTS

Direct verification of the prognostic free-air trajectories is rather difficult since the evaluation requires a detailed knowledge of the actual atmospheric motions. Most of the specialized techniques directed toward this problem involve the use of tracers, such as constant-level balloons or radioactive debris from nuclear tests, which are periodically sampled by radar and airborne sensors. However, such verification techniques are costly, limited in areal coverage, and difficult to carry out on a daily basis for a large number of forecasts. An indirect evaluation of the trajectory performance is obtained in the present research by verifying the 24-hr temperature and dew point forecasts at 1000, 850, 700 and 500 mb against actual RAOB reports. Forecast soundings at individual RAOB stations are constructed from the gridded forecasts by means of bi-linear interpolation. In mountainous areas, where the 1000-mb and 850-mb pressure surfaces are often below ground, the initial forecast level (mb) for the station sounding is derived from the smoothed terrain given in Fig. 3. The forecast soundings are subsequently verified for all upper-air stations located within the 13x17 subset of grid points given in Fig. 1. Each half of the grid is verified separately in order to distinguish between forecasts for mountainous areas and those for regions having relatively flat terrain. The eastern grid, with 35-40 stations reporting on the average, is composed of the eastern United States and Canada and the western grid, with 30-35 stations reporting, includes the western United States, southwestern Canada and northern Mexico. Temperature forecasts generated by the primitive equation model are verified in a similar manner to allow relative comparisons with the Lagrangian predictions.

Error field statistics compiled by the verification program include the mean absolute error (MABS), mean algebraic error (MALG) and the linear correlation coefficient (R) between forecast and observed values. The above statistics correspond to 24-hr forecasts verifying at 1800 CST, within the normal late afternoon period of maximum severe storm activity. Referring to Fig. 8, we find the MABS (eastern grid) plotted against pressure for the period May 1-July 31, 1968 (74 cases). As evidenced by Fig. 8, the Lagrangian temperature forecasts exhibit a relative improvement below 700 mb. The forecast refinement is most pronounced in the lowest 150 mb, where temperature and moisture distributions are critical to the development of severe storms. Above 700 mb, temperature forecasts from the primitive equation model are superior with an impressive 500-mb mean daily error of only 0.7C to 1.9C for the three-month verification period. A tentative examination of the 500-mb

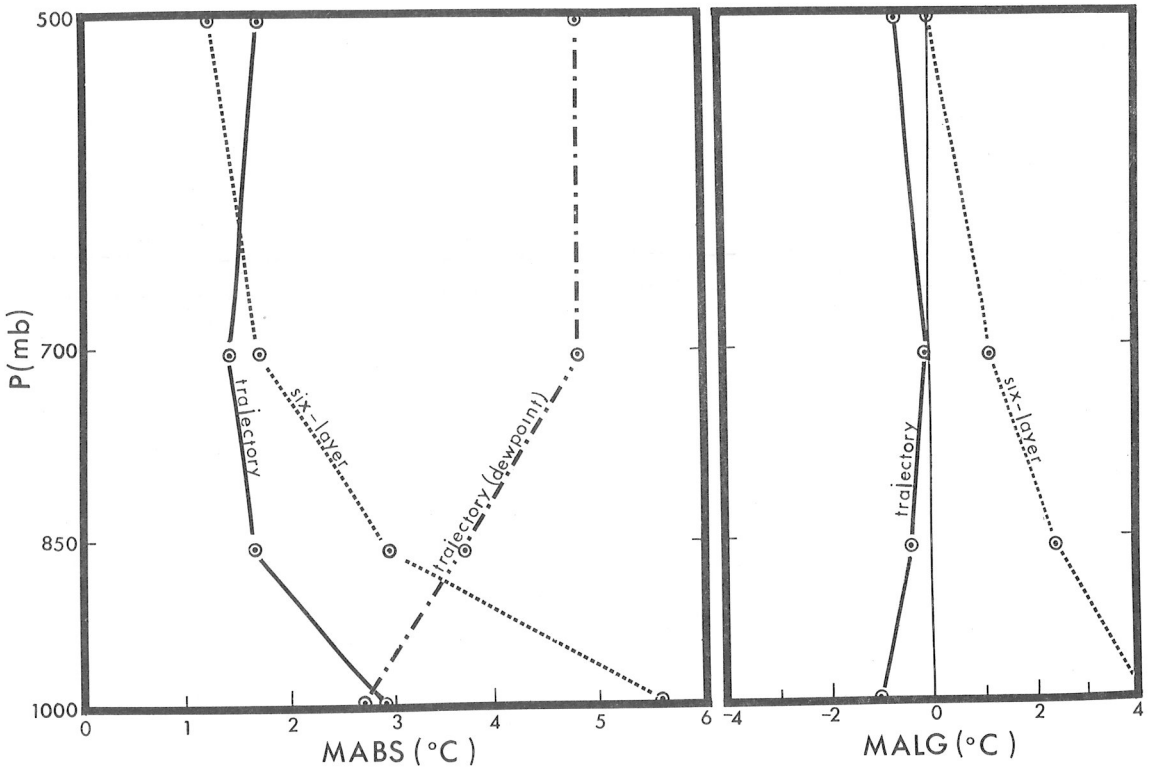

Figure 8. - Left, 24-hr mean absolute error for eastern grid temperature and dew point forecasts from May 1-July 31, 1968 (74 cases). Right, corresponding mean algebraic error for temperature forecasts.

error fields indicates that most of the significant errors in the trajectory forecasts result from trajectories originating over "silent" oceanic regions having few nearby observations.

The purpose of the MALG in Fig. 8 is to reveal any bias in either model to over or underforecast. The figure indicates that temperature forecasts from the primitive equation model are generally overforecast (too warm) below 500 mb, while the corresponding trajectory forecasts are, to a lesser degree, underforecast (too cold). The MALG is quite small for both models, indicating that the error distribution tends strongly toward the normal. Normalcy of the error curve is also evident from several frequency distributions, not reproduced here.

The dew point forecasts are verified against observed data only, since the primitive equation model does not output comparable moisture parameters at specific levels. An interesting feature shown by Fig. 8 is the similarity in the MABS for the 1000-mb temperature and dew point forecasts. However, the dew point error increases with height, in contrast to the temperature error. This is most probably due to the presence of pronounced moisture inversions or stratifications aloft which are absent at 1000 mb. For example, in several cases having sharp moisture inversions, an error of only 10-15 mb in forecasting the top of the moist layer resulted in errors of 15C-20C in the forecast dew points at the verification level. This type of error, while involving less than 2 percent of the stations verified, contributes

significantly to the observed increase in the MABS with height.

Table 1 lists the MALG, correlation coefficients, and percentages of explained variance for the eastern grid dew point forecasts. The most striking feature of the dew point verification is the tendency for the MALG to decrease linearly with pressure from a maximum error (too dry) at 1000 mb to zero near 500 mb. The underforecasting of both temperature and dew point in the lower levels by the trajectory program most likely results from neglecting the sensible heat flux and evaporative moisture flux from the ocean surface. Errors arising from the above effects are most pronounced in areas where the low-level trajectories terminate after a long over-water path with a large north-south component of motion. An air parcel following such a trajectory in the real atmosphere may originate from a relatively cold and dry land or oceanic region and in moving southward would subsequently pass over much warmer waters and undergo considerable modification.

TABLE 1. - MEAN ALGEBRAIC ERROR (MALG), LINEAR CORRELATION COEFFICIENT (R) AND PERCENTAGE OF EXPLAINED VARIANCE FOR EASTERN GRID DEW POINT FORECASTS (24 HR) FROM MAY 1-JULY 31, 1968 (74 CASES). THE MEAN STANDARD DEVIATION (σ) IS BASED ON 15 YEARS OF CLIMATOLOGICAL DATA (MAY-JULY) FOR 24 EASTERN GRID STATIONS.

	MALG	R	% EXP VAR	σ
1000	-1.9	0.93	87	-
850	-1.3	0.78	61	1.88
700	-0.6	0.67	45	2.03
500	0.0	0.64	41	1.97

Returning to Table 1, and examining the linear correlation coefficients and percentages of explained variance, we observe a marked trend in the performance of the trajectory moisture forecasts. A continuing decrease in forecast ability is indicated from the surface to 700 mb, above which little additional deterioration occurs. This decrease cannot be explained by a corresponding change in the observed dew point variability, as given in Table 1 by the mean standard deviations for May-July obtained from Crutcher and Meserve (1966). The deviations are based on 15 years of climatological data from 24 representative RAOB stations located in the eastern United States and Canada. As shown in Table 1, the standard deviations above 850 mb exhibit very little variation with height. Therefore, at first glance it appears reasonable to expect equal success in forecasting moisture patterns at 850 mb or 500 mb. Since this is obviously not the case, it is necessary to examine other pertinent aspects of the problem.

First, it must be recognized that all moisture above the contact layer in the real atmosphere is transported aloft by large-scale vertical motions, or in the convective case by vertical motions of a relatively intense and

localized nature. As previously described, the net vertical displacements computed by the trajectory program are derived from vertical velocity fields generated by the primitive equation model. However, the NMC fields are computed on a rather coarse grid, resulting in a significant amount of smoothing due to truncation. In comparison to the NMC estimates of vertical velocity, Danielsen (1966) and Nagle and Clark (1966) have obtained considerably larger values (2-3 times) from carefully constructed isentropic trajectories. Therefore, as given in Table 1, the moisture forecasts below 850 mb are quite satisfactory since the vertical motions are relatively weak and any corresponding errors in estimating the net vertical displacements are small. However, the errors in estimating the net vertical displacement become greater above 850 mb due to the normal increase in the large-scale vertical velocities with height and the neglect of localized convection. This leads to an underestimate of the vertical transport of moisture and a subsequent increase in the dew point error with height. In regions of pronounced moisture stratification, an underestimate in the large-scale vertical moisture transport is often reflected by an error in positioning the moist layer top. As previously discussed, this can occasionally result in rather large dew point errors involving specific levels at a few stations.

TABLE 2. - MEAN ABSOLUTE ERROR AND MEAN ALGEBRAIC ERROR (IN PARENTHESIS) FOR WESTERN GRID TEMPERATURE (T_A) AND DEW POINT (T_D) FORECASTS (24 HR) FROM MAY 1-JULY 31, 1968 (74 CASES).

	Six-Layer	Trajectory	
	T_A	T_A	T_D
1000	6.5(5.6)	3.5(-0.2)	4.3(-3.4)
850	3.3(2.2)	2.7(-0.3)	4.0(-1.0)
700	1.7(0.3)	1.8(0.1)	4.6(-1.7)
500	1.3(0.2)	1.9(-1.0)	5.1(-2.3)

Table 2 contains a summary of the verification statistics for the western grid temperature and dew point forecasts. In many respects the results are similar to those obtained for the eastern grid, as given in Fig. 8 and Table 1. Note the relative improvement shown by the trajectory temperature forecasts in the lower levels. The primitive equation model again exhibits a tendency to overforecast temperatures at 1000 mb and 850 mb, as given by the MALG in Table 2. However, the upper-level temperature forecasts generated by the primitive equation model are again superior to the trajectory forecasts. Most of the significant errors in the Lagrangian forecasts occur when the trajectories originate at a considerable distance from land over the data-sparse eastern Pacific Ocean. Speculation as to the reason for the relative success achieved in the upper levels by the primitive equation model centers on the incorporation of temperature "guess" fields in the objective analysis procedure. Such initial estimates, as derived from

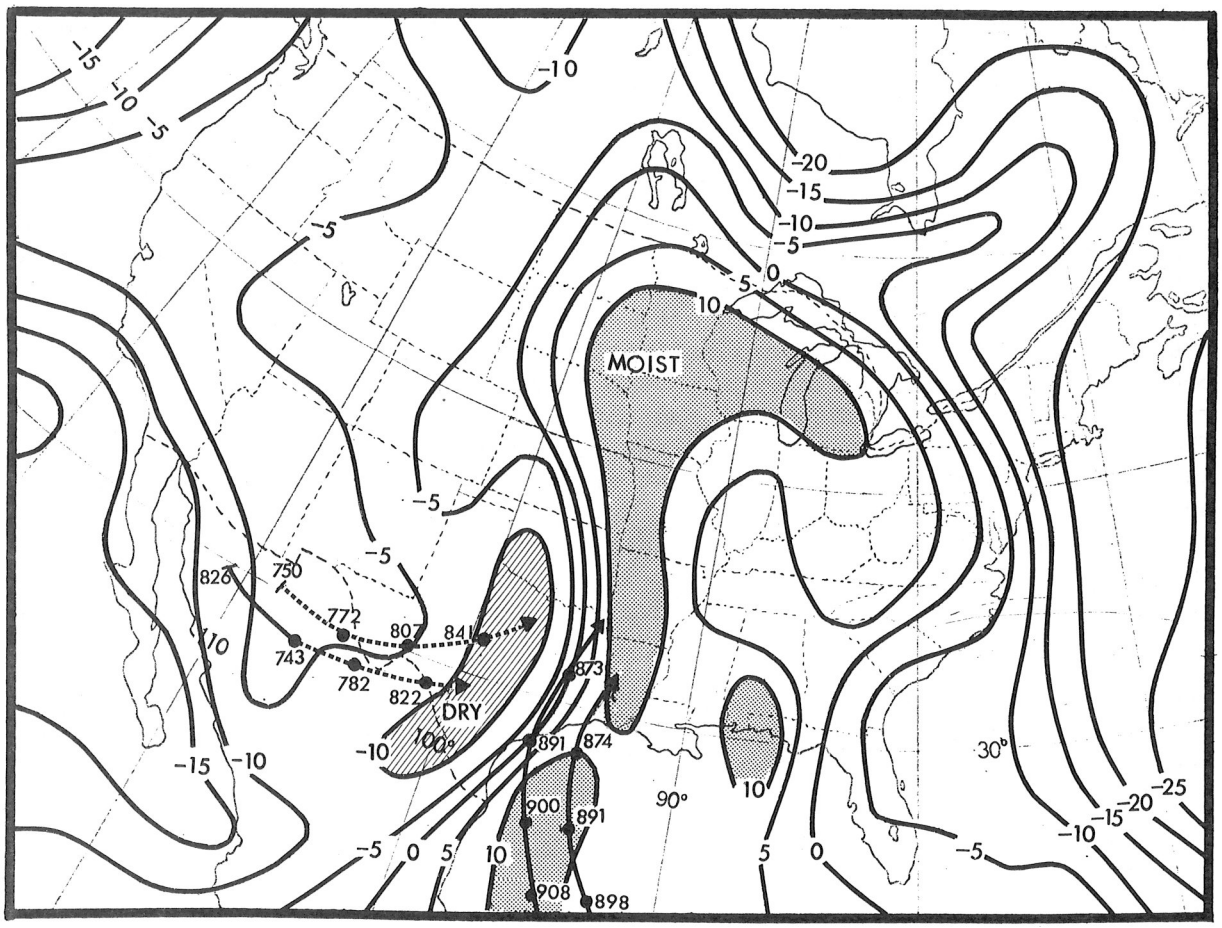

Figure 9. - 24-hr dew point forecast (°C) for 850 mb verifying at 0000 GMT April 14, 1967. Trajectories shown by solid (dashed) lines represent rising (subsiding) motion with pressures given at 6-hr intervals.

previous 12-hr height forecasts (Gustafson and McDonell, 1965), may be extremely important in determining the initial temperature distribution in oceanic regions where data are sparse or missing entirely. The larger dew point MABS in Table 2, as compared to Fig. 8, is also probably due in part to the relatively poor specification of moisture when the trajectory origin point is over the ocean.

Up to this point the dew point verification statistics are presented and discussed in a completely objective manner. An illustrative case study, typical of the majority of test cases with severe weather, is now briefly described to allow a somewhat more subjective insight into the character and quality of the forecast patterns and gradients. Referring to Fig. 9, we find a 24-hr dew point forecast for 850 mb verifying at 0000 GMT April 14, 1967. The forecast patterns at the end of the period represent a significant change from the initial dew point analysis, not reproduced here. As clearly shown by the low-level trajectories in Fig. 9, the pronounced gradients over eastern Texas and Oklahoma are created by the transport of air parcels from widely differing source regions. Warm and moist air rising from the Gulf of Mexico and dry subsiding air from extreme northwestern Mexico are observed to

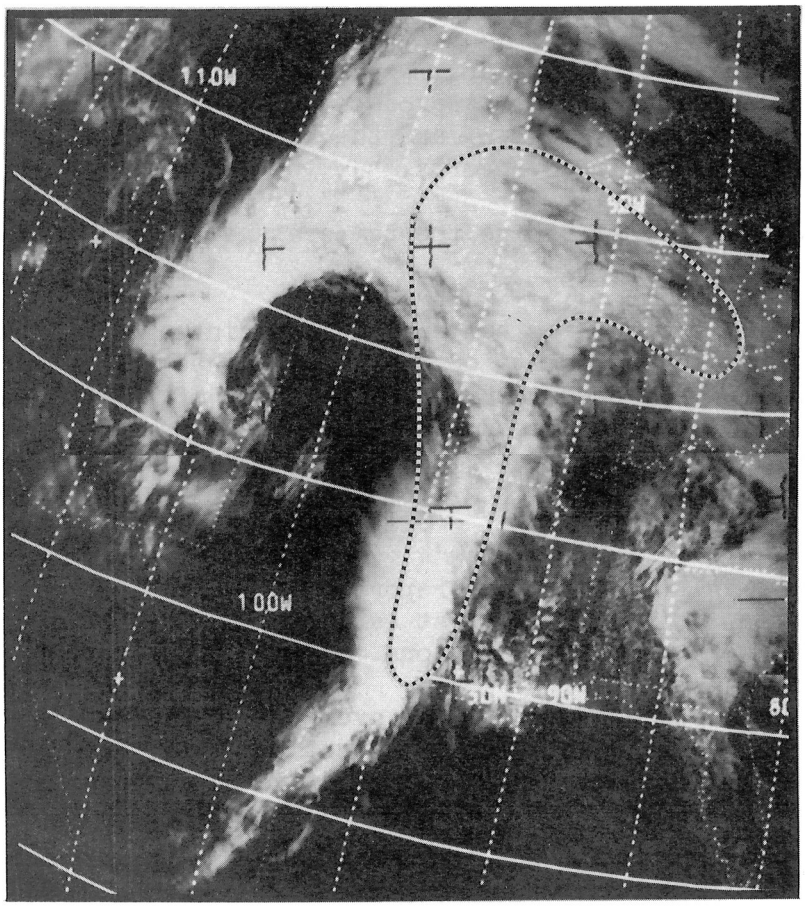

Figure 10. - ESSA 3 cloud photograph, orbit 2428, 1945 GMT April 13, 1967. The dashed line corresponds to the 10C isodrosotherm given in Fig. 9.

converge within a rather localized area (see Figs. 4-5). Numerous reports of tornadoes and funnel clouds were logged for this area and into extreme western Louisiana within four hours of the 0000 GMT verification time. The active squall line responsible for the severe weather outbreak is clearly indicated by the "bright area" in eastern Texas, as shown by the ESSA 3 cloud photograph (1945 GMT) given in Fig. 10. To assist in visually relating the cloud patterns in Fig. 10 to the dew point forecast in Fig. 9, note the 10C isodrosotherm on the satellite photograph. The coincidence between the instability line and the sharp moisture gradient is typical for most of the cases examined. Cirrus "blow-offs" from the squall line, resulting from horizontal wind shears aloft, are also quite evident in the photograph. Another interesting feature given in Fig. 10 is the extension of the cloud band over Colorado. However, this cloud pattern is associated with an upper-level circulation center and is not easily related to the moisture pattern at 850 mb.

7. CONCLUSIONS AND RECOMMENDATIONS

Significant improvements in the prediction of temperature and dew point at 1000 mb and 850 mb have been achieved by utilizing Eulerian wind forecasts as input data to a Lagrangian model. In the majority of cases with severe weather at verifying time, good agreement was found between the forecast dew point gradients and existing instability lines. The increased forecast

capability is in part made possible by supplementing the basic trajectory technique with additional refinements such as an improved terrain specification, an objective analysis scheme designed to reproduce detailed patterns and gradients at the point of trajectory origin, and the use of original upper-air data, including significant-level reports.

Specific recommendations to further refine the temperature and dew point forecasts are listed as follows:

1) Introduction of available sea-surface temperature data into the thermodynamic computations to provide an estimate of the sensible heat flux and evaporative moisture flux from the ocean surface. Inclusion of these effects, in the form of heat and moisture addition to the air parcels, would tend to reduce the bias (underforecast) observed in localized areas where the trajectories terminate after a long over-water path with a large north-south component of motion.

Diabatic Effects

2) A suitable statistical evaluation of ship-reported dew points, coupled with existing upper-air data, to provide a first estimate of the vertical moisture profiles over data-sparse oceanic regions.

3) The application of temperature "guess" fields over the ocean, as derived from previous 12-hr height forecasts. Such estimates can be extremely important in determining the initial temperature distribution when data is sparse or missing entirely.

8. ACKNOWLEDGMENTS

The author wishes to thank Drs. M. A. Alaka and H. R. Glahn of the Techniques Development Laboratory, Dr. J. D. Stackpole of the National Meteorological Center, Dr. W. Sangster of the Weather Bureau Central Region, and Mr. M. H. Kulawiec of the Weather Analysis and Prediction Division for their advice and assistance during the course of the work. Gratitude is also expressed to Mr. D. J. Foat, Mr. D. J. Sakelaris, and Miss L. Thompson for their assistance in preparing the manuscript.

REFERENCES

Angell, J. K: "An Analysis of 300 mb Transosonde Flights from Japan in 1957-58." Journal of Meteorology, Vol. 17, 20-35, 1960.

Berkofsky, L. and Bertoni, E. A: "Mean Topographic Charts for the Entire Earth." Bulletin of the American Meteorological Society, Vol. 36, 350-354, 1955.

Cressman, G. P: "An Operational Objective Analysis System." Monthly Weather Review, Vol. 87, 367-374, 1959.

Crutcher, H. L. and Meserve, J. M: "Selected Level Temperatures and Dew Points for the Northern Hemisphere." NAVAIR 50-1C-52, 1966.

Danielsen, E. F: "Trajectories: Isobaric, Isentropic and Actual." Journal of Meteorology, Vol. 18, 479-486, 1961.

Danielsen, E. F: "Research in Four-Dimensional Diagnosis of Cyclonic Storm Cloud Systems." Contract AF19(628)-4762, Scientific Report No. 2, Pennsylvania State University, 52 pp. 1966.

Djuric, D: "On the Accuracy of Air Trajectory Computations." Journal of Meteorology, Vol. 18, 597-605, 1961.

Edson, H., O'Neil, H. M. and Stephens, C. P: "Verification of Automated Temperature,Cloud and Wind Forecasts." Aerospace Sciences Technical Note 16, Headquarters 3d Weather Wing, USAF, 32 pp. 1967.

Endlich, R. M. and Mancuso, R. L: "Objective Analysis of Environmental Conditions Associated with Severe Thunderstorms and Tornadoes." Monthly Weather Review, Vol. 96, 342-350, 1968.

Gustafson, A. F. and McDonell, J. E: "Derivation of First Guess Fields for Objective Analyses, 1000 mb to 500 mb." NMC Technical Memorandum No. 31, 10 pp. 1965.

Murray, F. W: "On the Computation of Saturation Vapor Pressure." Journal of Applied Meteorology, Vol. 6, 203-204, 1967.

Nagle, R. E. and Clark, J. R: "Interpretative Uses of the Diagnostic-Cycle Routine." Final Report, Contract Cwb-11254, Meteorology International Incorporated, 43 pp. 1966.

Peterson, K. E: "Estimating Low-Level Tetroon Trajectories." Journal of Applied Meteorology, Vol. 5, 553-564, 1966.

Queney, P: "The Problem of Air Flow Over Mountains: A Summary of Theoretical Studies." Bulletin of the American Meteorological Society, Vol. 29, 16-26, 1948.

Rogers, C. W. and Sherr, P. E: "A Study of Dynamical Relationships between Cloud Patterns and Extratropical Cyclogenesis." Final Report, Contract E-47-67(N), Allied Research Associates, Incorporated, 74 pp. 1967.

Rossby, C. G: "Thermodynamics Applied to Air Mass Analysis." Massachusetts Institute of Technology Meteorological Papers, Vol. 1, 41 pp. 1932.

Shuman, F. G. and Hovermale, J. B: "An Operational Six-Layer Primitive Equation Model." Journal of Applied Meteorology, 1968, In Press.

Stackpole, J. D: "Numerical Analysis of Atmospheric Soundings." Journal of Applied Meteorology, Vol. 6, 464-467, 1967.